Current Distribution in the Electrodes of Industrial Three-phase Electric Smelting Furnaces

Author H. L. Larsen

Elkem AS Research
P.O.Box 5211 Majorstuen
NO-0303 Oslo, Norway
hilde-loken.larsen@elkem.no

Abstract: A 2D model for a cross section of the three electrodes in an industrial three-phase smelting furnace is made. The resulting current distribution within the electrodes is a function of the skin-effect within each electrode and the mutual influence between the magnetic fields of the electrode currents, the so-called proximity-effect.

Keywords: AC three-phase, Electric furnace, Skin-effect, Proximity effect

1. Introduction

Production of several metals, for instance various ferroalloys and silicon, take place in large industrial furnaces, see the sketch in Figure 1. The energy necessary for chemical reactions is supplied by three-phase alternating current through the three electrodes. Typically, the furnace power is 20 – 40 MW. The electrode current level is high, typically around 60 000 – 100 000 A, in each of the electrodes.
The process taking place within the furnace is truly multi-physics, with couplings between heat transfer, chemical reactions and electrical phenomena.

Some of the electrical issues involved are:

- The impedance (resistance and reactance) in the busbars and flexible cables between the transformers and the electrodes should ideally be equal for the three phases. In this way, the current supplied will be equal for the three phases. See an overview of the electrical system in Figure 2.
- The reactance is kept as low as possible in order to reduce the transformer size and fulfil requirements from power suppliers. The power factor of a furnace is typically around 0.7.
- Due to the high current level, current is also induced in surrounding equipment. This affects design and material choice, and shielding is sometimes necessary.
- Around the electrodes, current is supplied through vertical busbars, see Figure 1. Especially in self-baking electrodes, the current transfer to the electrodes should be as even as possible.
- A model of current distribution within the electrodes is presented in this paper.

In general, due to the large dimensions involved, combined with effects taking place in thin layers (for instance current transfer through the 3 – 5 mm steel shell surrounding the electrodes), meshing and computer limitations are often encountered.

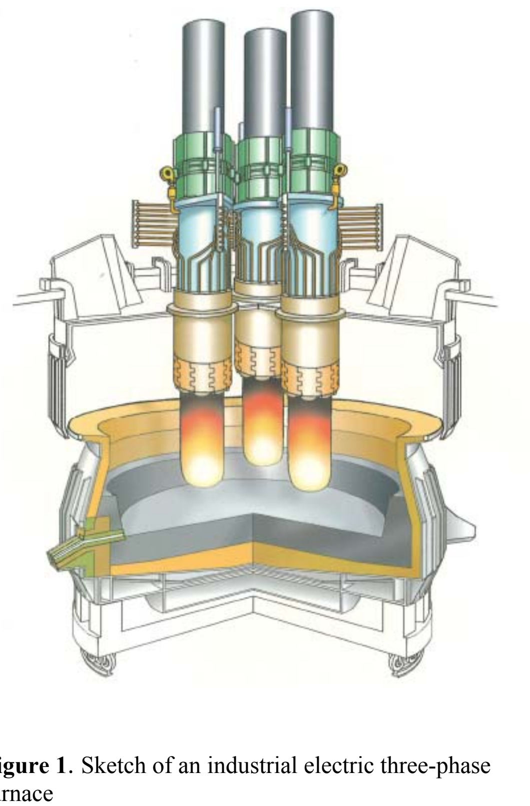

Figure 1. Sketch of an industrial electric three-phase furnace

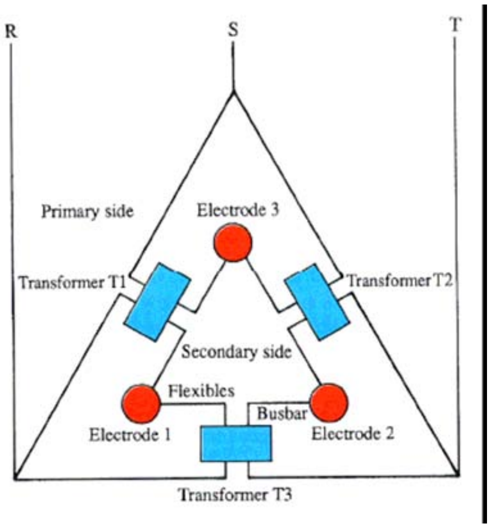

Figure 2. Three phase system of industrial furnaces

2. Current distribution in electrodes

The electrodes consist of graphite, or a self-baking carbon-containing electrodemass (the so-called "Søderberg"-electrode), alternatively a combination of the two in a composite electrode. The resulting current distribution within the electrodes is a result of the of the skin effect in each electrode combined with the mutual influence on neighbouring electrodes by the magnetic fields, the so-called "proximity effect".

As the current distribution within the electrodes affects the process conditions within the furnace, it is important to understand the fundamental effects that are involved.

In reality, the current distribution will also be affected by the temperature dependent electrical conductivity of the electrode materials. In addition to resistive heating, heat is also supplied by conduction from the hot furnace interior. However, this is not included in the present model.

3. Model

A 2D Femlab model, representing a cross section of the three electrodes, is set up. The frequency is 50 Hz, and the quasi-stationary approximation is valid. In the modelling example, the rms-value of the electrode currents is I = 80 000 A with 120^{o} phase delay among the electrodes. The electrical conductivity of the electrodes is set to σ = 30 000 $(\Omega m)^{-1}$.

The mode "Quasi-static, Magnetic - Perpendicular Induction Currents, Vector Potential" is used as the currents in this case are perpendicular to the modelling domain. The total electrode current is fixed, but induced currents contribute significantly to the total current. In order to handle this, a weak form point node is introduced.

Subdomain integration variables are used to integrate the total current density across each electrode. Each of the integration variables are then attached to a point. Through a test function, defined in the point, the total current is locked to the given one, which again is attached to each of the electrode subdomains.

In the model, the electrodes are surrounded by vacuum. On the boundary, the magnetic insulation condition is used. The relative magnetic permeability of all areas are μ_r = 1. The diameter of the modelling domain (Ø12 m) does not necessarily correspond to the furnace dimensions. The electrode diameter is 1.25 m.

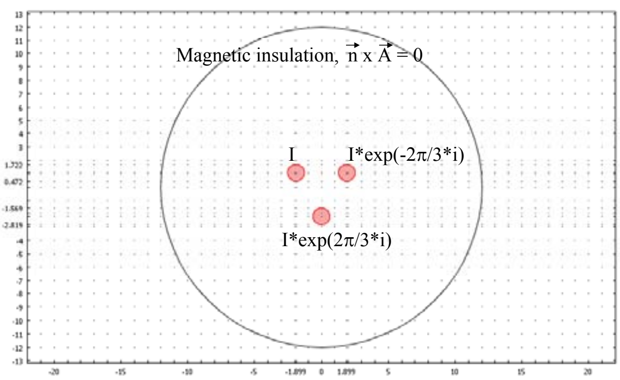

Figure 3. Modelling domain with boundary conditions

4. Results

4.1 Skin-effect in a single electrode

To see the effect of the skin effect in an electrode, the current in the neighbouring electrodes is set to zero. The resulting absolute values of the current density are seen in Figure 4, with the corresponding values through the electrode centre in Figure 5.

In this case, the skin depth is 0.41m. The skin-depth expression is based on a semi-infinite case, where the amplitude of the magnetic field is reduced to 37% of the value on the boundary a skin-depth away from the boundary. In this case with a circular electrode, the amplitude is reduced to approximately 31% a skin depth away from the boundary, as seen in Figure 6.

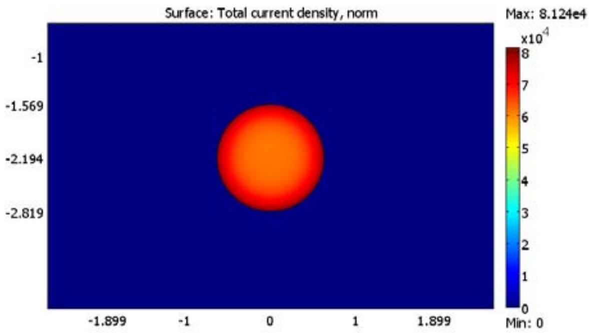

Figure 4. Absolute value of current density for one electrode due to skin effect

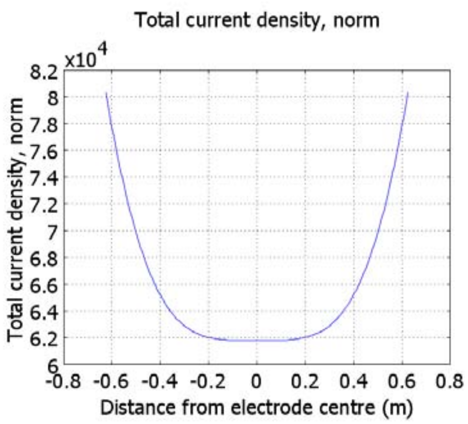

Figure 5. Absolute value of current density through the centre of an electrode

4.2 Combined skin- and proximity effect in three electrodes

The resulting absolute values of the current densities in the electrodes in the three-phase system are shown in Figure 7.

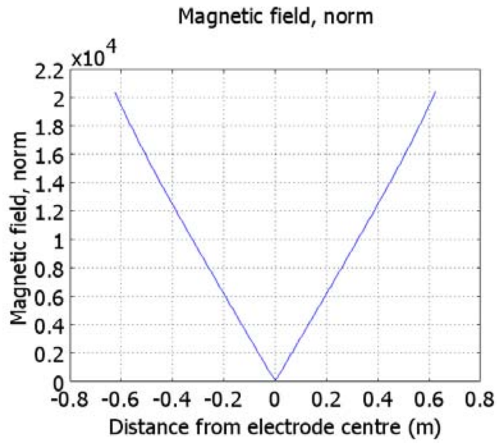

Figure 6. Absolute value of the magnetic field through the centre of an electrode

The resulting distribution is now a result of both the skin-effect and the “proximity” effect. The latter one is due to the fact that the magnetic fields are reducing each other be cause of the phase difference of 120°, and this effect is strongest in the parts of the electrodes with less distance to the neighbouring electrodes. Due to this effect, the reactance in parts of the electrodes is reduced, resulting in increased current densities in these parts.

It must be noted that the maximum current density is not towards the furnace centre, but towards the electrode which is 120° phase delayed (sequence 0°, 120°, -120°). This phenomena was early described theoretically by Dunski /1/, and also illustrated by Orth /2/. The resulting absolute value of current densities and the magnetic field through the centre of the upper right electrode in Figure 7, are shown in Figure 8 and 9.

In order to understand and interpret the furnace behaviour, it is important to have a clear picture of the basic electrical phenomena involved in deciding the current distribution within the electrodes. Especially for the self-baking electrodes, where the currents give rise to a “process taking part within the process”, this is valuable.

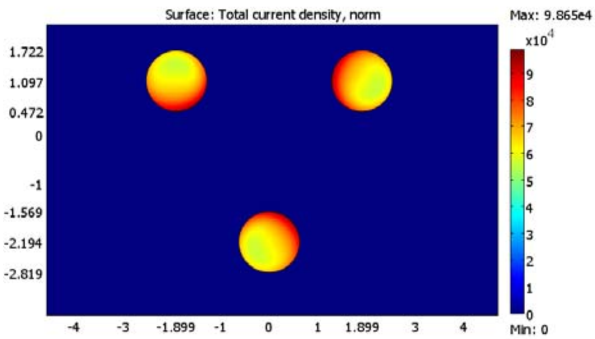

Figure 7. Absolute values of the current densities within the three electrodes.

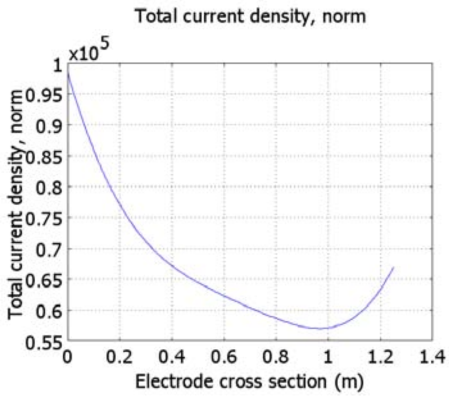

Figure 8. Absolute value of current density through the centre of an electrode

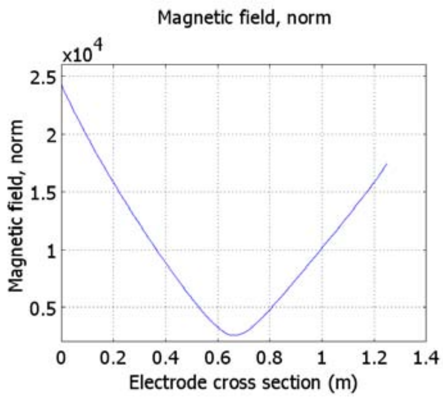

Figure 9. Absolute value of the magnetic field through the centre of an electrode

7. Conclusions

Although simplified, these types of models are useful in order to understand furnace behaviour in the three-phase industrial smelting furnaces. In general, Comsol Multiphysics offers a modelling tool well suited for the multi-physics nature of the processes taking place in industrial electric smelting furnaces.

8. References

1. Dunski, V.; Répartition du courant dans les électrodes d'un four triphasé à arcs en régimes équilibre et déséquilibré, Elektrowarme, Band 20, Nr. 12, p. 616 – 625, 1962
2. Orth, G.; Stromverdrängung in Graphitelektroden für Lichtbogenöfen, Elektrowärme International, 34, B1, p. 25 – 30.